Updated determination of light-cone distribution amplitudes of octet baryons in lattice QCD

G. S. Bali,[1] V. M. Braun,[1] S. Bürger,[1] M. Göckeler,[1,*] M. Gruber,[1] F. Kaiser,[1] B. A. Kniehl,[2] O. L. Veretin,[1,2] and P. Wein[1]

[1]*Institut für Theoretische Physik, Universität Regensburg, 93040 Regensburg, Germany*
[2]*II. Institut für Theoretische Physik, Universität Hamburg, 22761 Hamburg, Germany*

(Received 4 December 2024; accepted 2 May 2025; published 29 May 2025)

We present updated results for the wave function normalization constants and the first moments of the light-cone distribution amplitudes for the lowest-lying baryon octet. The analysis is carried out on a large number of $n_f = 2 + 1$ lattice gauge ensembles, including ensembles at physical pion (and kaon) masses. These are spread across five different lattice spacings, enabling a controlled continuum limit. The main differences with respect to our earlier work [G. S. Bali *et al.* (RQCD Collaboration), Light-cone distribution amplitudes of octet baryons from lattice QCD, Eur. Phys. J. A **55**, 116 (2019).] are the use of two-loop conversion factors to an $\overline{\text{MS}}$-like scheme and of an updated set of low-energy constants in the parametrization of the quark mass dependence. As a byproduct, for the first time, the anomalous dimensions for local leading-twist three-quark operators with one derivative are obtained.

DOI: 10.1103/PhysRevD.111.094517

I. INTRODUCTION

Light-cone distribution amplitudes (DAs) encode the distribution of the longitudinal momentum amongst the partons in the leading Fock states. They are probed in hard exclusive reactions, which involve large momentum transfer between the initial and final state hadron.

The evaluation of DAs from QCD is a challenging task, as they are genuinely nonperturbative objects. One possibility is the calculation of moments of DAs in lattice QCD. Results for the nucleon and hyperon DAs have been presented in several papers, e.g., Refs. [1,2]. For more recent discussions of other methods and the application to nucleon form factors, see Refs. [3–9]. The results given in Refs. [1,2] rely on the computation of hadronic matrix elements of local three-quark operators, which have to be renormalized. The standard renormalization procedure consists of two steps: the nonperturbative renormalization in a kind of momentum-subtraction scheme on the lattice is followed by a perturbative conversion in the continuum to an $\overline{\text{MS}}$-like scheme, which is more appropriate for phenomenological applications. Up to now, we had to limit ourselves to one-loop accuracy in the second step, due to the complexity of higher-loop calculations. However, it has been observed that in several cases the perturbative expansion of the (matrices of) conversion factors converges rather slowly. Therefore, we reanalyze here the data presented in Ref. [1] using two-loop conversion factors. For the operators without derivatives, these have been computed in Ref. [10]. The extension of these computations to operators with one derivative is part of the present paper. As a byproduct, we obtain the anomalous dimensions for twist-three three-quark operators with one derivative. In addition, we take the opportunity to update the values of the low-energy constants F_0, m_b, D, and F used in the analysis. For our final results, see Tables IV and V.

The paper is organized as follows. In Sec. II, we collect the relevant definitions, following Ref. [1]. In Sec. III, we sketch the analysis of our data, in particular, we discuss the changes in the renormalization procedure due to our two-loop calculation of the conversion matrices. We present our results in Sec. IV and compare them with the values obtained in Ref. [1].

Further technical details are given in the appendices. In Appendix A, we compile the three-quark operators used in the lattice computations. The two-loop conversion matrices for these operators are collected in Appendix B. Appendix C is devoted to the relevant (continuum) anomalous dimensions, in particular, we present the new two-loop contribution to the anomalous dimensions of twist-three operators with one derivative. The explicit form of the two-loop anomalous dimensions for our lattice operators with one derivative can be found in Appendix D. A direct comparison

*Contact author: meinulf.goeckeler@ur.de

of renormalization factors evaluated with the help of one-loop and two-loop conversion factors is shown in Appendix E.

II. THREE-QUARK DISTRIBUTION AMPLITUDES

Baryon DAs are defined as matrix elements of renormalized three-quark operators (we use the scheme proposed in Ref. [11]) at lightlike separations,

$$\begin{aligned}&\langle 0|[f_\alpha(a_1 n)g_\beta(a_2 n)h_\gamma(a_3 n)]^{\mathrm{R}}|B_{p,\lambda}\rangle\\&=\frac{1}{4}\int[dx]e^{-ip\cdot n\sum_i a_i x_i}\Big(v^B_{\alpha\beta;\gamma}V^B(x_1,x_2,x_3)\\&\quad+a^B_{\alpha\beta;\gamma}A^B(x_1,x_2,x_3)+t^B_{\alpha\beta;\gamma}T^B(x_1,x_2,x_3)+\cdots\Big).\end{aligned}\tag{1}$$

On the lhs, the Wilson lines as well as the color antisymmetrization are not written out explicitly but implied. The superscript R, indicating that the operator is renormalized, will be left out again in the following. The baryon state with momentum p and helicity λ is denoted by $|B_{p,\lambda}\rangle$, while α, β, γ are Dirac indices, n is a light-cone vector ($n^2=0$), and the a_i are real numbers. The quark fields f, g, h are of a given flavor matching the valence-quark content of the baryon B. Assuming isospin symmetry, we select one representative for each isospin multiplet, $N\equiv p$, $\Sigma\equiv\Sigma^-$, and $\Xi\equiv\Xi^0$,

B	f	g	h
N	u	u	d
Σ	d	d	s
Ξ	s	s	u
Λ	u	d	s.

On the rhs of Eq. (1), the integration measure for the longitudinal momentum fractions is given by

$$\int[dx]=\int_0^1 dx_1\int_0^1 dx_2\int_0^1 dx_3\,\delta(1-x_1-x_2-x_3).\tag{2}$$

Out of the 24 terms of the general Lorentz decomposition [12], we display in Eq. (1) only the three leading-twist (twist three) DAs, V^B, A^B, and T^B, which appear along with the structures

$$\begin{aligned}v^B_{\alpha\beta;\gamma}&=(\tilde{\not n}C)_{\alpha\beta}(\gamma_5 u^{B,+}_{p,\lambda})_\gamma,\\a^B_{\alpha\beta;\gamma}&=(\tilde{\not n}\gamma_5 C)_{\alpha\beta}(u^{B,+}_{p,\lambda})_\gamma,\\t^B_{\alpha\beta;\gamma}&=(i\sigma_{\perp\tilde n}C)_{\alpha\beta}(\gamma^\perp\gamma_5 u^{B,+}_{p,\lambda})_\gamma.\end{aligned}\tag{3}$$

Here, C is the charge conjugation matrix and we use the notation

$$\begin{aligned}\sigma_{\perp\tilde n}\otimes\gamma^\perp&=\sigma^{\mu\rho}\tilde n_\rho g^\perp_{\mu\nu}\otimes\gamma^\nu,\\g^\perp_{\mu\nu}&=g_{\mu\nu}-\frac{\tilde n_\mu n_\nu+\tilde n_\nu n_\mu}{\tilde n\cdot n},\\u^{B,+}_{p,\lambda}&=\frac{1}{2}\frac{\tilde{\not n}\not n}{\tilde n\cdot n}u^B_{p,\lambda},\\\tilde n_\mu&=p_\mu-\frac{1}{2}\frac{m_B^2}{p\cdot n}n_\mu,\end{aligned}\tag{4}$$

where $u^B_{p,\lambda}$ is the Dirac spinor with on-shell momentum p and helicity λ.

It proves convenient to define the following set of DAs:

$$\begin{aligned}\Phi^{B\neq\Lambda}_\pm(x_{123})&=\frac{1}{2}\Big([V-A]^B(x_{123})\pm[V-A]^B(x_{321})\Big),\\\Pi^{B\neq\Lambda}(x_{123})&=T^B(x_{132}),\\\Phi^\Lambda_+(x_{123})&=\sqrt{\frac{1}{6}}\Big([V-A]^\Lambda(x_{123})+[V-A]^\Lambda(x_{321})\Big),\\\Phi^\Lambda_-(x_{123})&=-\sqrt{\frac{3}{2}}\Big([V-A]^\Lambda(x_{123})-[V-A]^\Lambda(x_{321})\Big),\\\Pi^\Lambda(x_{123})&=\sqrt{6}T^\Lambda(x_{132}),\end{aligned}\tag{5}$$

with the abbreviation $(x_{ijk})\equiv(x_i,x_j,x_k)$. Using the phase conventions for the baryon states and the corresponding flavor wave functions detailed in Appendix A of Ref. [2], the following relations hold in the limit of SU(3) flavor symmetry (subsequently indicated by a $\star$), where $m_u=m_d=m_s$:

$$\begin{aligned}&\Phi^\star_+\equiv\Phi^{N\star}_+=\Phi^{\Sigma\star}_+=\Phi^{\Xi\star}_+=\Phi^{\Lambda\star}_+=\Pi^{N\star}=\Pi^{\Sigma\star}=\Pi^{\Xi\star},\\&\Phi^\star_-\equiv\Phi^{N\star}_-=\Phi^{\Sigma\star}_-=\Phi^{\Xi\star}_-=\Phi^{\Lambda\star}_-=\Pi^{\Lambda\star}.\end{aligned}\tag{6}$$

In the case of SU(2) isospin symmetry, which is exact in our $N_f=2+1$ simulation ($m_u=m_d\equiv m_\ell$) and is only broken very mildly in the real world, the nucleon DA Π^N is equal to Φ^N_+ in the whole m_ℓ-m_s-plane.

DAs can be expanded in terms of orthogonal polynomials $\mathcal{P}_{nk}$ [13] in such a way that the coefficients have autonomous scale dependence at one loop. For the DAs defined in Eq. (5), this expansion reads

$$\begin{aligned}\Phi^B_+&=120x_1x_2x_3(\varphi^B_{00}\mathcal{P}_{00}+\varphi^B_{11}\mathcal{P}_{11}+\cdots),\\\Phi^B_-&=120x_1x_2x_3(\varphi^B_{10}\mathcal{P}_{10}+\cdots),\\\Pi^{B\neq\Lambda}&=120x_1x_2x_3(\pi^B_{00}\mathcal{P}_{00}+\pi^B_{11}\mathcal{P}_{11}+\cdots),\\\Pi^\Lambda&=120x_1x_2x_3(\pi^\Lambda_{10}\mathcal{P}_{10}+\cdots).\end{aligned}\tag{7}$$

In this way, all nonperturbative information is encoded in the set of scale-dependent coefficients φ^B_{nk}, π^B_{nk} (also called

shape parameters), which can be related to matrix elements of local operators that are calculable on the lattice. The first few polynomials are

$$\begin{aligned}\mathcal{P}_{00} &= 1,\\ \mathcal{P}_{10} &= 21(x_1 - x_3),\\ \mathcal{P}_{11} &= 7(x_1 - 2x_2 + x_3).\end{aligned} \tag{8}$$

The leading contributions in Eq. (7) are $120x_1x_2x_3\varphi_{00}^B$ and $120x_1x_2x_3\pi_{00}^{B\neq\Lambda}$. They are usually referred to as the asymptotic DAs. The corresponding normalization coefficients φ_{00}^B and $\pi_{00}^{B\neq\Lambda}$ can be thought of as the wave functions at the origin. They are also denoted as f^B and $f_T^{B\neq\Lambda}$,

$$f^B = \varphi_{00}^B, \qquad f_T^{B\neq\Lambda} = \pi_{00}^B. \tag{9}$$

Using chiral quark fields $q^{\uparrow\downarrow} = \frac{1}{2}(\mathbb{1} \pm \gamma_5)q$ and baryon spinors $u_{p,\lambda}^{B\uparrow\downarrow} = \frac{1}{2}(\mathbb{1} \pm \gamma_5)u_{p,\lambda}^B$, they can be expressed as matrix elements of local currents with all quark fields taken at the origin,

$$\begin{aligned}\langle 0|(f^{\uparrow T}C\not{n}g^{\downarrow})\not{n}h^{\uparrow}|(B\neq\Lambda)_{p,\lambda}\rangle &= -\frac{1}{2}f^B p\cdot n\not{n}u_{p,\lambda}^{B\uparrow},\\ \langle 0|(u^{\uparrow T}C\not{n}d^{\downarrow})\not{n}s^{\uparrow}|\Lambda_{p,\lambda}\rangle &= -\sqrt{\frac{3}{8}}f^\Lambda p\cdot n\not{n}u_{p,\lambda}^{\Lambda\uparrow},\\ \langle 0|(f^{\uparrow T}C\gamma^\mu\not{n}g^{\uparrow})\gamma_\mu\not{n}h^{\downarrow}|(B\neq\Lambda)_{p,\lambda}\rangle &= 2f_T^B p\cdot n\not{n}u_{p,\lambda}^{B\uparrow}.\end{aligned} \tag{10}$$

In the limit of isospin symmetry, these two couplings coincide for the nucleon, $f_T^N = f^N$, see, e.g., Ref. [14]. For the Λ baryon, the zeroth moment of T^Λ vanishes by construction so that only one leading-twist normalization constant f^Λ exists.

We also consider normalized first moments of $[V-A]^B$ and $T^{B\neq\Lambda}$,

$$\begin{aligned}\langle x_i\rangle^B &= \frac{1}{f^B}\int[dx]x_i[V-A]^B,\\ \langle x_i\rangle_T^{B\neq\Lambda} &= \frac{1}{f_T^B}\int[dx]x_i T^B,\end{aligned} \tag{11}$$

which can be computed from the shape parameters:

$$\begin{aligned}\langle x_1\rangle^{B\neq\Lambda} &= \frac{1}{3} + \frac{1}{3}\hat{\varphi}_{11}^B + \hat{\varphi}_{10}^B,\\ \langle x_2\rangle^{B\neq\Lambda} &= \frac{1}{3} - \frac{2}{3}\hat{\varphi}_{11}^B,\\ \langle x_3\rangle^{B\neq\Lambda} &= \frac{1}{3} + \frac{1}{3}\hat{\varphi}_{11}^B - \hat{\varphi}_{10}^B,\\ \langle x_1\rangle_T^{B\neq\Lambda} &= \frac{1}{3} + \frac{1}{3}\hat{\pi}_{11}^B,\\ \langle x_2\rangle_T^{B\neq\Lambda} &= \frac{1}{3} + \frac{1}{3}\hat{\pi}_{11}^B,\\ \langle x_3\rangle_T^{B\neq\Lambda} &= \frac{1}{3} - \frac{2}{3}\hat{\pi}_{11}^B,\\ \langle x_1\rangle^{\Lambda} &= \frac{1}{3} + \frac{1}{3}\hat{\varphi}_{11}^\Lambda - \frac{1}{3}\hat{\varphi}_{10}^\Lambda,\\ \langle x_2\rangle^{\Lambda} &= \frac{1}{3} - \frac{2}{3}\hat{\varphi}_{11}^\Lambda,\\ \langle x_3\rangle^{\Lambda} &= \frac{1}{3} + \frac{1}{3}\hat{\varphi}_{11}^\Lambda + \frac{1}{3}\hat{\varphi}_{10}^\Lambda,\end{aligned} \tag{12}$$

where

$$\hat{\varphi}_{nk}^B = \frac{\varphi_{nk}^B}{f^B}, \qquad \hat{\pi}_{11}^{B\neq\Lambda} = \frac{\pi_{11}^B}{f_T^B}. \tag{13}$$

Loosely speaking, one can interpret these moments as fractions of the baryon's total momentum carried by the individual valence quarks, e.g., $\langle x_1\rangle^N$ corresponds to the momentum fraction carried by the spin-up u quark $u^\uparrow$ in the nucleon, $\langle x_2\rangle^N$ corresponds to the momentum fraction carried by the spin-down u quark $u^\downarrow$, etc. These assignments will be indicated in the tables showing our results for these moments.

The 21 DAs of higher twist [indicated in Eq. (1) by the ellipsis on the rhs] only involve two new normalization constants (λ_1^B and λ_2^B) for the isospin-nonsinglet baryons (N, Σ, Ξ) and three (λ_1^Λ, λ_T^Λ, and λ_2^Λ) for the Λ baryon. These can be defined as matrix elements of local three-quark twist-four operators without derivatives,

$$\begin{aligned}\langle 0|(f^{\uparrow T}C\gamma^\mu g^{\downarrow})\gamma_\mu h^{\uparrow}|(B\neq\Lambda)_{p,\lambda}\rangle &= -\frac{1}{2}\lambda_1^B m_B u_{p,\lambda}^{B\downarrow},\\ \langle 0|(f^{\uparrow T}C\sigma^{\mu\nu}g^{\uparrow})\sigma_{\mu\nu}h^{\uparrow}|(B\neq\Lambda)_{p,\lambda}\rangle &= \lambda_2^B m_B u_{p,\lambda}^{B\uparrow},\\ \langle 0|(u^{\uparrow T}C\gamma^\mu d^{\downarrow})\gamma_\mu s^{\uparrow}|\Lambda_{p,\lambda}\rangle &= \frac{1}{2\sqrt{6}}\lambda_1^\Lambda m_\Lambda u_{p,\lambda}^{\Lambda\downarrow},\\ \langle 0|(u^{\uparrow T}Cd^{\uparrow})s^{\downarrow}|\Lambda_{p,\lambda}\rangle &= \frac{1}{2\sqrt{6}}\lambda_T^\Lambda m_\Lambda u_{p,\lambda}^{\Lambda\downarrow},\\ \langle 0|(u^{\uparrow T}Cd^{\uparrow})s^{\uparrow}|\Lambda_{p,\lambda}\rangle &= \frac{-1}{4\sqrt{6}}\lambda_2^\Lambda m_\Lambda u_{p,\lambda}^{\Lambda\uparrow}.\end{aligned} \tag{14}$$

The definitions are chosen such that in the flavor symmetric limit,

$$\lambda_1^\star \equiv \lambda_1^{N\star} = \lambda_1^{\Sigma\star} = \lambda_1^{\Xi\star} = \lambda_1^{\Lambda\star} = \lambda_T^{\Lambda\star},$$
$$\lambda_2^\star \equiv \lambda_2^{N\star} = \lambda_2^{\Sigma\star} = \lambda_2^{\Xi\star} = \lambda_2^{\Lambda\star}. \quad (15)$$

III. DATA ANALYSIS

We strictly follow the procedure described in Ref. [1]. In particular, we work with the same set of gauge configurations generated within the Coordinated Lattice Simulations effort [15] with $n_f = 2 + 1$ dynamical quarks. We also use the same lattice operators as in Refs. [1,2], collected in Appendix A, and perform the renormalization as described in Ref. [1]. We first calculate the renormalization and mixing coefficients nonperturbatively within a (regularization-independent) momentum-subtraction scheme adapted to the case of three-quark operators. These coefficients are subsequently converted to the $\overline{\text{MS}}$-like scheme suggested in Ref. [11] with the help of (continuum) perturbation theory. In Ref. [1], we had only one-loop results at our disposal, while we can now make use of our new two-loop conversion matrices (see Appendix B). We perform several fits to the scale dependence of the resulting numbers, extract the renormalization matrices at the target scale of 2 GeV from each of these fits, and use them in independent analyses of the physical quantities to obtain the final values and systematic uncertainties of our results. The essential elements of the fits are collected in Table I, which supersedes Table 1 in Ref. [1]. Here, μ_1 is the initial scale of the fit range, the loop order of the conversion matrices is given by n_{loops}, and n_{disc} denotes the number of terms in the parametrization of the lattice artifacts. As we have updated the scales following Ref. [16], the uncertainty due to the scale setting is now reduced to 1.2% (from 3% in Ref. [1]) and the value of λ^2_{scale} in fit 5 has been changed accordingly. Finally, $\Lambda^{(3)}_{\overline{\text{MS}}} = 341(12)$ MeV [17] is varied within its uncertainty. Also, the pion masses used for the chiral extrapolations have changed slightly. Further technical details of our renormalization procedure can be found in Ref. [18].

The two-loop calculation of the conversion matrices has been performed with the help of dimensional regularization employing standard techniques. However, for three-quark operators there are subtleties due to contributions of evanescent operators that have to be taken into account. We employ the renormalization scheme suggested in Ref. [11] (see also Ref. [19]). In a first step, we use integration by parts to reduce the Feynman integrals to a smaller set of so-called master integrals (four integrals at one-loop order and 44 integrals at two-loop order). These master integrals are then evaluated numerically. The details of the calculation in the case of the operators without derivatives can be found in Ref. [10]. Notice that the number of spin tensor structures to be considered in the calculation increases from 581 for the operators without derivatives to 2895 for the operators with one derivative.

TABLE I. Fit choices regarding the determination of the renormalization and mixing factors.

Fit	μ_1^2 [GeV^2]	n_{loops}	n_{disc}	λ^2_{scale}	$\Lambda^{(3)}_{\overline{\text{MS}}}$ [MeV]
1	4	2	3	1.0	341
2	10	2	3	1.0	341
3	4	1	3	1.0	341
4	4	2	2	1.0	341
5	4	2	3	1.012	341
6	4	2	3	1.0	353

The uncertainties due to the numerical integration amount to at most a few permille in the two-loop conversion coefficients. For our final results, they are completely negligible.

As a byproduct of these computations we also obtain the two-loop anomalous dimensions of the twist-three three-quark operators with one derivative that have not been known previously, see Appendix C. Notice that in the case of the operators without derivatives, even the three-loop anomalous dimensions are known [19]. For the operators with one derivative that are used in the lattice calculations of baryon DAs, we collect the anomalous dimensions in Appendix D. Numerical values of the two-loop conversion matrices for the operators and the momentum configuration employed in Refs. [1,2,18] can be found in Appendix B. We stress that the anomalous dimensions beyond one-loop order and the conversion matrices starting at one loop are scheme dependent. Our results are based on the renormalization scheme of Ref. [11].

While in most cases the perturbative expansion of the conversion matrices shows the expected behavior with a two-loop correction that is smaller than the one-loop contribution for reasonably large scales, there are a few cases where either the one-loop term is unusually small and the two-loop term is of a reasonable size or the two-loop correction is considerably smaller than the one-loop contribution. In Fig. 1 we show examples for these two situations (operators without derivatives $\mathcal{O}_1^{12}$ and $\mathcal{S}_1^A$ in the notation of Ref. [18], see also Appendix A) as well as for the usual behavior (multiplet $\mathcal{S}_2^{12}$ of operators with one derivative).

In all the cases, the scale dependence of the renormalization and mixing coefficients obtained with two-loop conversion looks rather satisfactory in the sense that after rescaling to the target scale of 2 GeV the data tend to develop approximate plateaus as the lattice spacing decreases (i.e., as β increases). (Notice, however, the cautionary remarks at the end of Sec. VII in Ref. [18].) This can be seen in Figs. 2–4, where we display the resulting renormalization factors evaluated either with the one-loop or the two-loop conversion factor. Given the conversion factors shown in the middle panel of Fig. 1, it is not

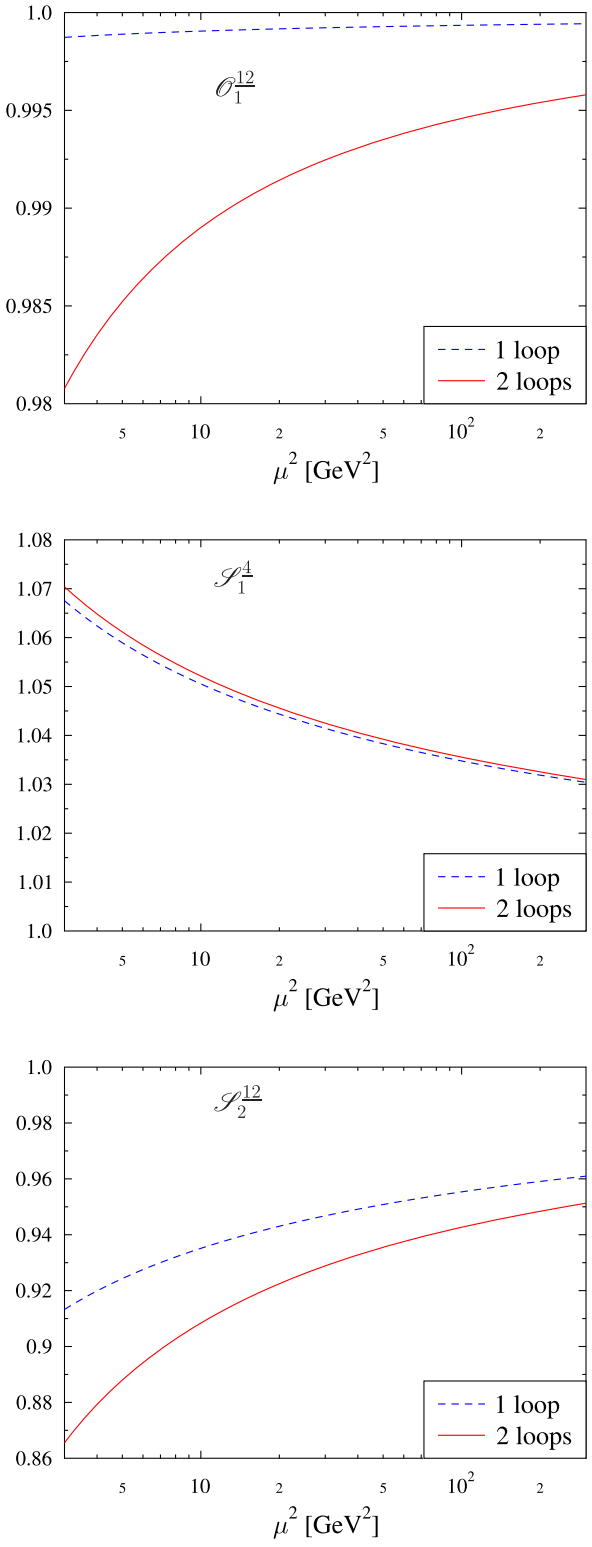

FIG. 1. Conversion factors for the multiplets $\mathcal{O}_1^{12}$, $\mathcal{S}_1^4$, and $\mathcal{S}_2^{12}$ in the one- and two-loop approximation. The tree-level results equal 1.

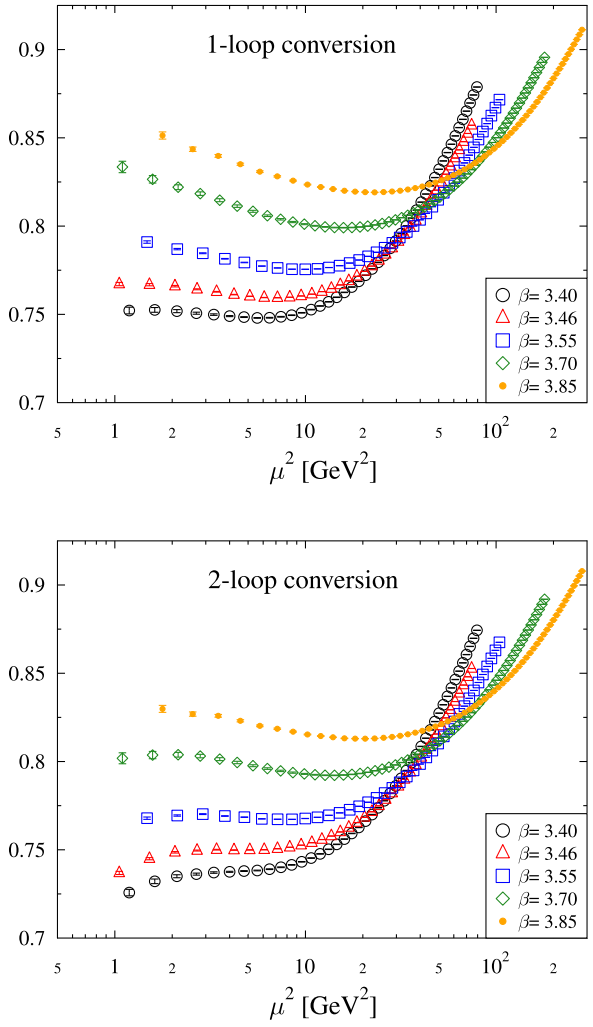

FIG. 2. Renormalization factor for the multiplet $\mathcal{O}_1^{12}$ rescaled to the target scale of 2 GeV computed with the help of the one-loop (top panel) and the two-loop (bottom panel) conversion factor. In both cases, the three-loop anomalous dimension has been used. The coupling $\beta = 3.4(3.85)$ corresponds to the coarsest (finest) lattice spacing $a = 0.085(0.039)$ fm, employed here, see Refs. [1,16].

surprising that the two plots in Fig. 3 are hardly distinguishable, where the upper plot shows the same data as Fig. 4 in Ref. [1]. For an easier comparison of the effect of one-loop and two-loop conversion, we plot some of the data presented in Figs. 2 and 4 in a different form in Appendix E.

IV. RESULTS

Presenting our results, we begin with the numbers obtained with the two-loop conversion matrices (factors) and the values for the low-energy constants F_0, m_b, D, and F used in the original article [1]: $F_0 = 87$ MeV, $D = 0.623$, $F = 0.441$, and $m_b = 880$ MeV (taken from Ref. [20]). Hence, the only difference with the old results is the use of the two-loop conversion instead of the one-loop approximation.

We collect our results in Tables II and III. The comparison with the results of Ref. [1] in these tables highlights the

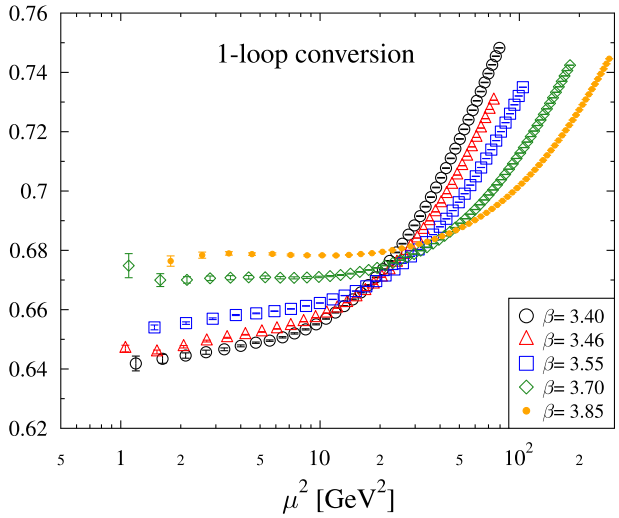

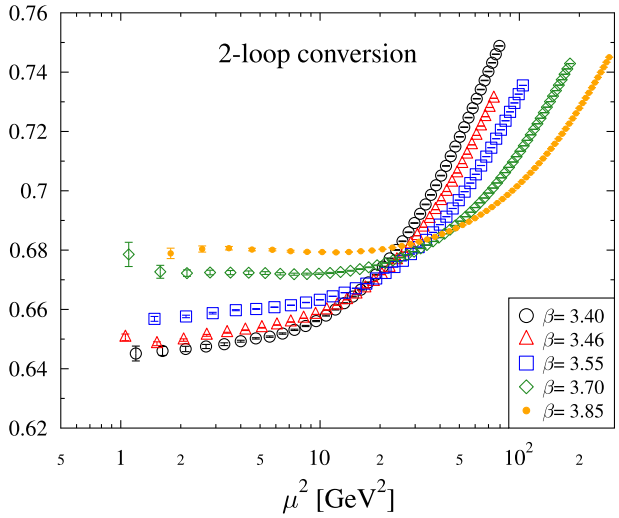

FIG. 3. Renormalization factor for the multiplet $\mathscr{S}_1^4$ rescaled to the target scale of 2 GeV computed with the help of the one-loop (top panel) and the two-loop (bottom panel) conversion factor. In both cases, the three-loop anomalous dimension has been used.

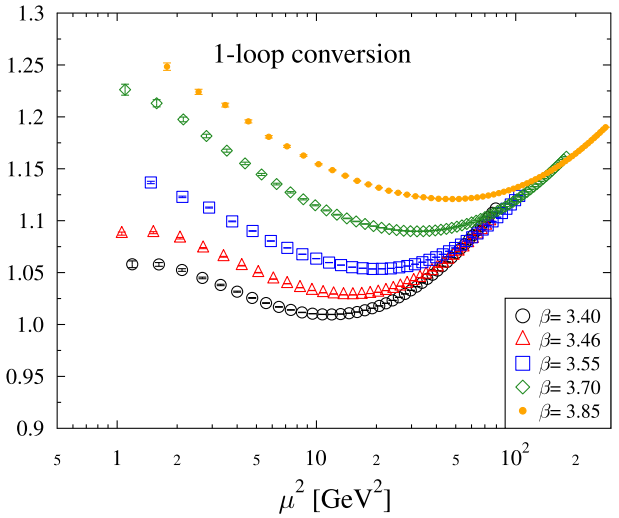

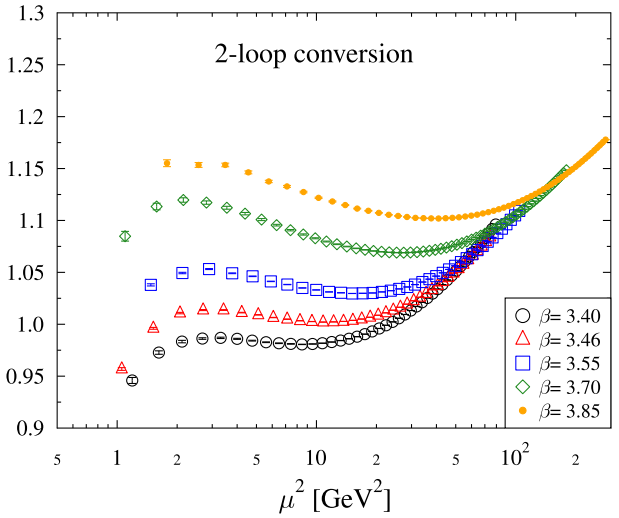

FIG. 4. Renormalization factor for the multiplet $\mathscr{S}_2^{12}$ rescaled to the target scale of 2 GeV computed with the help of the one-loop (top panel) and the two-loop (bottom panel) conversion factor. In both cases, the two-loop anomalous dimension has been used.

effect of increasing the loop order of the conversion. Recall that (as in Ref. [1]) the systematic error due to the chiral extrapolation has been estimated by including higher-order terms in the chiral expansion. Table II (Table III) corresponds to Table 2 (Table 4) of Ref. [1].

Comparing old and new results, one observes that replacing the one-loop conversion matrices with the corresponding two-loop approximations does not lead to significant changes in our results. Therefore, the perturbative uncertainties for the quantities considered here seem to be under control. While the central values change only marginally, the estimates of the errors due to the renormalization (r) are in general reduced, sometimes significantly, as one could have anticipated. Somewhat surprising is the effect seen in the errors related to the continuum extrapolation (a). For the coupling constants, i.e., for f^B, f_T^B, λ_1^B, λ_T^B, and λ_2^B, these uncertainties are reduced. However, for most of the shape parameters they are increased, in some cases even considerably. Perhaps this different behavior is related to the fact that the coupling constants are computed from operators without derivatives [cf. Eqs. (10) and (14)], while the evaluation of the shape parameters involves operators with one derivative, which are generally more difficult to handle.

At first sight, it might be surprising that the differences between the results obtained with one-loop and two-loop conversion are smaller than one might have expected from, e.g., Fig. 4. However, one has to take into account that the values of the renormalization coefficients that we finally use are not simply read off from curves, such as those shown in Figs. 2–4, but result from fits to the scale dependence. Furthermore, because SU(3) flavor symmetry

TABLE II. Results for the couplings and shape parameters using two-loop conversion factors, compared to the values obtained with one-loop conversion from Ref. [1]. For this comparison, we employ the "old" values of the low-energy constants taken from Ref. [20]. All quantities are given in units of 10^{-3} GeV^2 in our $\overline{\text{MS}}$-like scheme at a scale $\mu = 2$ GeV with three active quark flavors. The superscripts and subscripts denote the statistical error after extrapolation to the physical point. The numbers in parentheses give estimates for the systematic errors due to renormalization (r), continuum extrapolation (a), and chiral extrapolation (m). Due to the scale setting uncertainty, the new (old) results carry an additional error of 1.2% (3%), which is not displayed.

B	N	Σ	Ξ	Λ
f^B	$3.55^{+6}_{-4}(1)_r(0)_a(0)_m$	$5.32^{+5}_{-5}(2)_r(0)_a(5)_m$	$6.14^{+7}_{-7}(2)_r(0)_a(15)_m$	$4.89^{+7}_{-4}(2)_r(0)_a(6)_m$
[1]	$3.54^{+6}_{-4}(1)_r(2)_a(0)_m$	$5.31^{+5}_{-4}(1)_r(3)_a(4)_m$	$6.11^{+7}_{-6}(2)_r(4)_a(13)_m$	$4.87^{+7}_{-4}(2)_r(3)_a(5)_m$
f_T^B	$3.55^{+6}_{-4}(1)_r(0)_a(0)_m$	$5.15^{+5}_{-4}(2)_r(0)_a(5)_m$	$6.32^{+8}_{-7}(2)_r(0)_a(16)_m$	
[1]	$3.54^{+6}_{-4}(1)_r(2)_a(0)_m$	$5.14^{+5}_{-4}(1)_r(3)_a(3)_m$	$6.29^{+8}_{-7}(1)_r(4)_a(15)_m$	
φ_{11}^B	$0.125^{+6}_{-5}(7)_r(23)_a(0)_m$	$0.203^{+4}_{-6}(9)_r(44)_a(0)_m$	$-0.001^{+4}_{-3}(12)_r(0)_a(0)_m$	$0.250^{+8}_{-7}(9)_r(49)_a(0)_m$
[1]	$0.118^{+6}_{-5}(8)_r(21)_a(0)_m$	$0.195^{+4}_{-6}(10)_r(40)_a(0)_m$	$-0.014^{+4}_{-3}(18)_r(3)_a(0)_m$	$0.243^{+8}_{-7}(9)_r(46)_a(0)_m$
π_{11}^B	$0.125^{+6}_{-5}(7)_r(23)_a(0)_m$	$-0.077^{+2}_{-2}(11)_r(16)_a(0)_m$	$0.405^{+7}_{-9}(9)_r(86)_a(0)_m$	
[1]	$0.118^{+6}_{-5}(8)_r(21)_a(0)_m$	$-0.090^{+3}_{-2}(17)_r(18)_a(0)_m$	$0.399^{+7}_{-9}(9)_r(81)_a(0)_m$	
φ_{10}^B	$0.184^{+20}_{-14}(2)_r(8)_a(1)_m$	$0.091^{+12}_{-24}(2)_r(5)_a(0)_m$	$0.351^{+19}_{-21}(5)_r(20)_a(1)_m$	$0.606^{+21}_{-27}(7)_r(30)_a(2)_m$
[1]	$0.182^{+20}_{-14}(6)_r(4)_a(1)_m$	$0.090^{+11}_{-31}(3)_r(3)_a(1)_m$	$0.350^{+18}_{-20}(11)_r(11)_a(1)_m$	$0.610^{+23}_{-28}(18)_r(16)_a(2)_m$
π_{10}^B				$0.218^{+32}_{-27}(3)_r(12)_a(2)_m$
[1]				$0.214^{+33}_{-26}(7)_r(6)_a(2)_m$
λ_1^B	$-45.5^{+1.1}_{-1.0}(0.3)_r(2.8)_a(0.6)_m$	$-46.9^{+0.9}_{-0.9}(0.3)_r(2.8)_a(0.5)_m$	$-50.5^{+0.8}_{-1.0}(0.3)_r(3.3)_a(0.3)_m$	$-42.9^{+0.8}_{-0.8}(0.4)_r(2.5)_a(0.5)_m$
[1]	$-44.9^{+1.2}_{-0.9}(0.9)_r(3.9)_a(0.6)_m$	$-46.1^{+1.0}_{-0.9}(0.9)_r(4.1)_a(0.5)_m$	$-49.8^{+0.8}_{-0.9}(1.0)_r(4.7)_a(0.2)_m$	$-42.2^{+0.8}_{-0.8}(0.9)_r(3.7)_a(0.4)_m$
λ_T^B				$-53.1^{+1.1}_{-1.1}(0.4)_r(3.4)_a(0.4)_m$
[1]				$-52.3^{+1.2}_{-1.0}(1.1)_r(4.7)_a(0.3)_m$
λ_2^B	$95.0^{+2.3}_{-2.3}(0.5)_r(3.2)_a(1.4)_m$	$86.7^{+1.9}_{-1.7}(0.2)_r(3.0)_a(1.2)_m$	$100.9^{+2.4}_{-1.8}(0.3)_r(3.7)_a(1.1)_m$	$100.3^{+2.5}_{-2.2}(0.6)_r(3.5)_a(1.3)_m$
[1]	$93.4^{+2.3}_{-2.2}(1.7)_r(3.7)_a(1.2)_m$	$85.2^{+1.8}_{-1.7}(1.6)_r(3.4)_a(1.3)_m$	$99.5^{+2.3}_{-1.8}(1.9)_r(4.3)_a(1.1)_m$	$98.9^{+2.4}_{-2.1}(1.9)_r(4.1)_a(1.1)_m$

is broken, renormalization coefficients of different operators (which may behave differently when the order of the perturbative expansion is increased) enter the evaluation of the physical quantities.

TABLE III. Results (using two-loop conversion factors) for the normalized first moments (11) of the DAs $[V-A]^B$ and $T^{B\neq\Lambda}$, compared to the values obtained with one-loop conversion from Ref. [1]. For this comparison, we employ the "old" values of the low-energy constants taken from Ref. [20]. The results refer to our $\overline{\text{MS}}$-like scheme at a scale $\mu = 2$ GeV. All uncertainties from our calculation have been added in quadrature.

B	N		Σ		Ξ		Λ	
$\langle x_1\rangle^B$	$u^\uparrow$	0.397^{+7}_{-6}	$d^\uparrow$	0.363^{+4}_{-6}	$s^\uparrow$	0.391^{+5}_{-5}	$u^\uparrow$	0.309^{+2}_{-2}
[1]	$u^\uparrow$	0.396^{+7}_{-6}	$d^\uparrow$	0.363^{+4}_{-7}	$s^\uparrow$	0.390^{+4}_{-4}	$u^\uparrow$	0.308^{+3}_{-3}
$\langle x_2\rangle^B$	$u^\downarrow$	0.310^{+5}_{-5}	$d^\downarrow$	0.308^{+6}_{-6}	$s^\downarrow$	0.333^{+1}_{-1}	$d^\downarrow$	0.299^{+7}_{-7}
[1]	$u^\downarrow$	0.311^{+5}_{-5}	$d^\downarrow$	0.309^{+5}_{-5}	$s^\downarrow$	0.335^{+2}_{-2}	$d^\downarrow$	0.300^{+7}_{-7}
$\langle x_3\rangle^B$	$d^\uparrow$	0.293^{+4}_{-5}	$s^\uparrow$	0.329^{+5}_{-3}	$u^\uparrow$	0.276^{+5}_{-5}	$s^\uparrow$	0.392^{+6}_{-6}
[1]	$d^\uparrow$	0.293^{+5}_{-6}	$s^\uparrow$	0.329^{+6}_{-3}	$u^\uparrow$	0.275^{+5}_{-5}	$s^\uparrow$	0.392^{+5}_{-5}
$\langle x_1\rangle_T^B$	$u^\uparrow$	0.345^{+2}_{-2}	$d^\uparrow$	0.328^{+1}_{-1}	$s^\uparrow$	0.355^{+5}_{-5}		
[1]	$u^\uparrow$	0.344^{+2}_{-2}	$d^\uparrow$	0.327^{+2}_{-2}	$s^\uparrow$	0.354^{+5}_{-5}		
$\langle x_2\rangle_T^B$	$u^\uparrow$	0.345^{+2}_{-2}	$d^\uparrow$	0.328^{+1}_{-1}	$s^\uparrow$	0.355^{+5}_{-5}		
[1]	$u^\uparrow$	0.344^{+2}_{-2}	$d^\uparrow$	0.327^{+2}_{-2}	$s^\uparrow$	0.354^{+5}_{-5}		
$\langle x_3\rangle_T^B$	$d^\downarrow$	0.310^{+5}_{-5}	$s^\downarrow$	0.343^{+2}_{-2}	$u^\downarrow$	0.291^{+9}_{-9}		
[1]	$d^\downarrow$	0.311^{+5}_{-5}	$s^\downarrow$	0.345^{+3}_{-3}	$u^\downarrow$	0.291^{+9}_{-9}		

In the case of meson DAs [21], the effects related to the order of the perturbative conversion are of a similar size as those found here, if one considers the first moments. However, for the second Gegenbauer moment, the effect is more pronounced. Presumably, the second moments of the baryon DAs are also more sensitive to the order of the perturbative conversion.

A more recent analysis [16] obtained somewhat different central values for the low-energy constants that enter the chiral extrapolation: $F_0 = 71.1$ MeV, $D = 0.57$, $F = 0.34$, and $m_b = 821$ MeV. We repeated our fits using these new numbers as input (along with the two-loop conversion matrices). As some results changed by an amount that was considerably larger than the estimate of the systematic uncertainty due to the chiral extrapolation determined as in Ref. [1], we modified this estimate by adding in quadrature the error evaluated according to the previous procedure and the difference in the results. The corresponding numbers can be found in Tables IV and V, which are our final results. Table IV (Table V) is to be compared with Table 2 (Table 4) of Ref. [1]. Notice that due to the scale setting uncertainty [16], all new results in Tables II and IV carry an additional error of 1.2%, while the scale setting error of the old results in Table II amounts to 3%. The dimensionless quantities displayed in Tables III and V are not affected by this uncertainty.

TABLE IV. Final results for the couplings and shape parameters, using the low-energy constants from Ref. [16] and two-loop conversion factors. All values are given in units of 10^{-3} GeV^2 in our $\overline{\text{MS}}$-like scheme at a scale $\mu = 2$ GeV with three active quark flavors. The superscripts and subscripts denote the statistical error after extrapolation to the physical point. The values in parentheses give estimates for the systematic errors due to renormalization (r), continuum extrapolation (a), and chiral extrapolation (m). The latter error is estimated according to the modified procedure described in the text. Due to the scale setting uncertainty, all results carry an additional error of 1.2% (not displayed).

B	N	Σ	Ξ	Λ
f^B	$3.29^{+6}_{-4}(1)_r(1)_a(26)_m$	$5.32^{+5}_{-5}(2)_r(2)_a(9)_m$	$6.15^{+8}_{-7}(2)_r(3)_a(25)_m$	$4.75^{+6}_{-4}(2)_r(2)_a(16)_m$
f_T^B	$3.29^{+6}_{-4}(1)_r(1)_a(26)_m$	$5.15^{+5}_{-4}(2)_r(2)_a(9)_m$	$6.34^{+8}_{-8}(3)_r(3)_a(26)_m$	
φ_{11}^B	$0.118^{+6}_{-4}(7)_r(21)_a(7)_m$	$0.200^{+4}_{-6}(10)_r(42)_a(3)_m$	$-0.001^{+4}_{-3}(12)_r(0)_a(0)_m$	$0.242^{+8}_{-6}(9)_r(46)_a(8)_m$
π_{11}^B	$0.118^{+6}_{-4}(7)_r(21)_a(7)_m$	$-0.080^{+2}_{-2}(12)_r(16)_a(3)_m$	$0.399^{+7}_{-9}(9)_r(82)_a(6)_m$	
φ_{10}^B	$0.181^{+19}_{-15}(2)_r(7)_a(3)_m$	$0.094^{+10}_{-42}(2)_r(4)_a(3)_m$	$0.361^{+16}_{-27}(5)_r(19)_a(10)_m$	$0.563^{+33}_{-27}(6)_r(27)_a(43)_m$
π_{10}^B				$0.237^{+30}_{-35}(4)_r(12)_a(19)_m$
λ_1^B	$-44.3^{+1.0}_{-1.0}(0.3)_r(3.3)_a(1.4)_m$	$-47.6^{+0.9}_{-0.9}(0.3)_r(3.7)_a(1.1)_m$	$-50.2^{+0.7}_{-0.9}(0.3)_r(4.1)_a(0.8)_m$	$-44.0^{+0.7}_{-0.8}(0.5)_r(3.3)_a(1.3)_m$
λ_T^B				$-54.2^{+1.1}_{-1.1}(0.3)_r(4.3)_a(1.4)_m$
λ_2^B	$97.2^{+1.9}_{-2.7}(1.2)_r(1.2)_a(2.4)_m$	$85.8^{+2.0}_{-1.4}(0.8)_r(0.4)_a(2.2)_m$	$101.4^{+2.3}_{-1.9}(0.2)_r(1.1)_a(1.3)_m$	$99.7^{+2.3}_{-2.4}(0.6)_r(1.2)_a(1.3)_m$

TABLE V. Final results for the normalized first moments (11) of the DAs $[V-A]^B$ and $T^{B\neq\Lambda}$, using the low-energy constants from Ref. [16] and two-loop conversion factors. The results refer to our $\overline{\text{MS}}$-like scheme at a scale $\mu = 2$ GeV. All uncertainties from our calculation have been added in quadrature, including the differences with the central values given in Table III.

B	N		Σ		Ξ		Λ	
$\langle x_1\rangle^B$	$u^\uparrow$	0.400^{+9}_{-8}	$d^\uparrow$	0.363^{+4}_{-9}	$s^\uparrow$	0.392^{+5}_{-6}	$u^\uparrow$	0.311^{+3}_{-4}
$\langle x_2\rangle^B$	$u^\downarrow$	0.309^{+5}_{-5}	$d^\downarrow$	0.308^{+6}_{-6}	$s^\downarrow$	0.333^{+1}_{-1}	$d^\downarrow$	0.299^{+7}_{-7}
$\langle x_3\rangle^B$	$d^\uparrow$	0.290^{+6}_{-7}	$s^\uparrow$	0.328^{+8}_{-3}	$u^\uparrow$	0.275^{+6}_{-5}	$s^\uparrow$	0.390^{+6}_{-6}
$\langle x_1\rangle_T^B$	$u^\uparrow$	0.345^{+2}_{-2}	$d^\uparrow$	0.328^{+1}_{-1}	$s^\uparrow$	0.354^{+5}_{-5}		
$\langle x_2\rangle_T^B$	$u^\uparrow$	0.345^{+2}_{-2}	$d^\uparrow$	0.328^{+1}_{-1}	$s^\uparrow$	0.354^{+5}_{-5}		
$\langle x_3\rangle_T^B$	$d^\downarrow$	0.309^{+5}_{-5}	$s^\downarrow$	0.344^{+3}_{-3}	$u^\downarrow$	0.291^{+9}_{-9}		

ACKNOWLEDGMENTS

This work was supported by the Deutsche Forschungsgemeinschaft [Research Unit FOR 2926 (project 40824754) and PUNCH4NFDI (project 460248186)]. Additional support from the European Union's Horizon 2020 Research and Innovation Programme under the Marie Skłodowska-Curie Grant Agreement No. 813942 (ITN EuroPLEx) and Grant Agreement No. 824093 (STRONG 2020) is gratefully acknowledged. We used a modified version of the CHROMA [22] software package along with the LIBHADRONANALYSIS library and improved inverters [23–26]. We thank all our Coordinated Lattice Simulations [15,27] colleagues for the joint generation of the gauge ensembles, using OPENQCD [24,28]. The computation of observables was carried out on the QPACE 2 and QPACE 3 systems, on the Regensburg HPC-cluster ATHENE 2, and at various supercomputer centers. In particular, the authors gratefully acknowledge computer time granted by the John von Neumann Institute for Computing (NIC), provided on the Booster partition of the supercomputer JURECA [29] at Jülich Supercomputing Centre (JSC) [30] and granted by the Gauss Centre for Supercomputing (GCS) on JUWELS [31] at JSC. GCS is the alliance of the three national supercomputing centres HLRS (Universität Stuttgart), JSC (Forschungszentrum Jülich), and LRZ (Bayerische Akademie der Wissenschaften), funded by the German Federal Ministry of Education and Research (BMBF) and the German State Ministries for Research of Baden-Württemberg (MWK), Bayern (StMWFK), and Nordrhein-Westfalen (MIWF).

DATA AVAILABILITY

The data that support the findings of this article are not publicly available. The data are available from the authors upon reasonable request.

APPENDIX A: THREE-QUARK OPERATOR MULTIPLETS

In lattice computations, it is convenient to employ operator multiplets that transform irreducibly not only with respect to the lattice symmetry, the spinorial hypercubic group $\overline{\text{H}(4)}$, but also with respect to the group $\mathcal{S}_3$ of permutations of the three quark flavors. The latter group has three nonequivalent irreducible representations, which we label by the names of the corresponding ground state particle multiplets in a flavor symmetric world. Therefore, the one-dimensional trivial representation is labeled by $\mathscr{D}$, the one-dimensional totally antisymmetric representation by $\mathscr{S}$, and the two-dimensional representation by $\mathscr{O}$. Out of the irreducible representations of $\overline{\text{H}(4)}$, only the spinorial representations are relevant for three-quark operators. They are called τ_1^4, τ_2^4, τ^8, τ_1^{12}, and τ_2^{12}, where the superscript

indicates the dimension and the subscript distinguishes inequivalent representations of the same dimension (see, e.g., Ref. [32]).

We construct multiplets with the desired transformation properties from the multiplets defined in Ref. [32]. For operators without derivatives in the representation τ_1^{12} of $\overline{\mathrm{H}(4)}$, we have one doublet of operator multiplets transforming according to the two-dimensional representation of $\mathcal{S}_3$,

$$\mathscr{O}_{\bar{1}}^{12} = \begin{Bmatrix} \frac{1}{\sqrt{6}}(\mathcal{O}_7 + \mathcal{O}_8 - 2\mathcal{O}_9) \\ \frac{1}{\sqrt{2}}(\mathcal{O}_7 - \mathcal{O}_8) \end{Bmatrix}, \tag{A1}$$

and one operator multiplet transforming trivially under $\mathcal{S}_3$,

$$\mathscr{D}_{\bar{1}}^{12} = \frac{1}{\sqrt{3}}(\mathcal{O}_7 + \mathcal{O}_8 + \mathcal{O}_9). \tag{A2}$$

For operators without derivatives in the $\overline{\mathrm{H}(4)}$ representation τ_1^4, we have one multiplet that is totally antisymmetric under flavor permutations,

$$\mathscr{S}_{\bar{1}}^{4} = \frac{1}{\sqrt{3}}(\mathcal{O}_3 - \mathcal{O}_4 - \mathcal{O}_5), \tag{A3}$$

and two doublets of operator multiplets transforming according to the two-dimensional representation of $\mathcal{S}_3$,

$$(\mathscr{O}_{\bar{1}}^{4})_1 = \begin{Bmatrix} \frac{1}{\sqrt{2}}(\mathcal{O}_3 + \mathcal{O}_4) \\ \frac{1}{\sqrt{6}}(-\mathcal{O}_3 + \mathcal{O}_4 - 2\mathcal{O}_5) \end{Bmatrix}, \tag{A4}$$

$$(\mathscr{O}_{\bar{1}}^{4})_2 = \begin{Bmatrix} \mathcal{O}_2 \\ \frac{1}{\sqrt{3}}(2\mathcal{O}_1 + \mathcal{O}_2) \end{Bmatrix}. \tag{A5}$$

In the case of operators with one derivative, we restrict ourselves to multiplets that transform according to the $\overline{\mathrm{H}(4)}$ representation τ_2^{12}, because only these are safe from mixing with lower-dimensional operators. There are twelve linearly independent multiplets with this transformation behavior [32]. In Appendix A. 2 of Ref. [32] one can find explicit expressions for four multiplets, labeled $\mathcal{O}_{D5}$, $\mathcal{O}_{D6}$, $\mathcal{O}_{D7}$, and $\mathcal{O}_{D8}$, where the derivative acts on the third quark field. As the transformation properties of the operators do not depend on the position of the derivative, the remaining eight multiplets can be constructed by moving the derivative to the second or to the first quark field. In the following, we replace the D by f, g, or h in order to indicate on which quark field the covariant derivative acts: f (g, h) means that the derivative acts on the first (second, third) quark field.

In this way, we get one multiplet that is totally antisymmetric under $\mathcal{S}_3$,

$$\mathscr{S}_{\bar{2}}^{12} = \frac{1}{\sqrt{6}}[(\mathcal{O}_{g5} - \mathcal{O}_{h5}) + (\mathcal{O}_{h6} - \mathcal{O}_{f6}) + (\mathcal{O}_{f7} - \mathcal{O}_{g7})]. \tag{A6}$$

Additionally, there are four doublets of operator multiplets corresponding to the two-dimensional representation of $\mathcal{S}_3$,

$$(\mathscr{O}_{\bar{2}}^{12})_1 = \begin{Bmatrix} \frac{1}{3\sqrt{2}}[(\mathcal{O}_{f5} + \mathcal{O}_{g5} + \mathcal{O}_{h5}) + (\mathcal{O}_{f6} + \mathcal{O}_{g6} + \mathcal{O}_{h6}) - 2(\mathcal{O}_{f7} + \mathcal{O}_{g7} + \mathcal{O}_{h7})] \\ \frac{1}{\sqrt{6}}[(\mathcal{O}_{f5} + \mathcal{O}_{g5} + \mathcal{O}_{h5}) - (\mathcal{O}_{f6} + \mathcal{O}_{g6} + \mathcal{O}_{h6})] \end{Bmatrix}, \tag{A7}$$

$$(\mathscr{O}_{\bar{2}}^{12})_2 = \begin{Bmatrix} \frac{1}{6}[(-2\mathcal{O}_{f5} + \mathcal{O}_{g5} + \mathcal{O}_{h5}) + (\mathcal{O}_{f6} - 2\mathcal{O}_{g6} + \mathcal{O}_{h6}) - 2(\mathcal{O}_{f7} + \mathcal{O}_{g7} - 2\mathcal{O}_{h7})] \\ \frac{1}{2\sqrt{3}}[(-2\mathcal{O}_{f5} + \mathcal{O}_{g5} + \mathcal{O}_{h5}) - (\mathcal{O}_{f6} - 2\mathcal{O}_{g6} + \mathcal{O}_{h6})] \end{Bmatrix}, \tag{A8}$$

$$(\mathscr{O}_{\bar{2}}^{12})_3 = \begin{Bmatrix} \frac{1}{2}[(\mathcal{O}_{g5} - \mathcal{O}_{h5}) - (\mathcal{O}_{h6} - \mathcal{O}_{f6})] \\ \frac{1}{2\sqrt{3}}[(\mathcal{O}_{h5} - \mathcal{O}_{g5}) + (\mathcal{O}_{f6} - \mathcal{O}_{h6}) - 2(\mathcal{O}_{g7} - \mathcal{O}_{f7})] \end{Bmatrix}, \tag{A9}$$

$$(\mathscr{O}_{\bar{2}}^{12})_4 = \begin{Bmatrix} \frac{1}{\sqrt{6}}(\mathcal{O}_{f8} + \mathcal{O}_{g8} - 2\mathcal{O}_{h8}) \\ \frac{1}{\sqrt{2}}(\mathcal{O}_{f8} - \mathcal{O}_{g8}) \end{Bmatrix}, \tag{A10}$$

and three operator multiplets transforming trivially under flavor permutations,

$$(\mathscr{D}_{\bar{2}}^{12})_1 = \frac{1}{3}[(\mathcal{O}_{f5} + \mathcal{O}_{g5} + \mathcal{O}_{h5}) + (\mathcal{O}_{f6} + \mathcal{O}_{g6} + \mathcal{O}_{h6}) + (\mathcal{O}_{f7} + \mathcal{O}_{g7} + \mathcal{O}_{h7})], \tag{A11}$$

$$(\mathscr{D}^{12}_{\bar{2}})_2 = \frac{1}{3\sqrt{2}}[(-2\mathcal{O}_{f5} + \mathcal{O}_{g5} + \mathcal{O}_{h5}) + (\mathcal{O}_{f6} - 2\mathcal{O}_{g6} + \mathcal{O}_{h6}) + (\mathcal{O}_{f7} + \mathcal{O}_{g7} - 2\mathcal{O}_{h7})], \tag{A12}$$

$$(\mathscr{D}^{12}_{\bar{2}})_3 = \frac{1}{\sqrt{3}}(\mathcal{O}_{f8} + \mathcal{O}_{g8} + \mathcal{O}_{h8}). \tag{A13}$$

APPENDIX B: CONVERSION MATRICES FOR LATTICE OPERATORS

In this appendix we collect numerical values for the two-loop conversion matrices of the three-quark operators used in the lattice calculations. They refer to the momentum configuration employed in our renormalization condition on the lattice, where we used the following momenta (in Euclidean space) for the three external quark lines:

$$\begin{aligned} p_1 &= \frac{\mu}{2}(+1,+1,+1,+1), \\ p_2 &= \frac{\mu}{2}(-1,-1,-1,+1), \\ p_3 &= \frac{\mu}{2}(+1,-1,-1,-1). \end{aligned} \tag{B1}$$

Notice that the scale μ will drop out in the coefficients of the perturbative expansion of the conversion matrices. Analytical expressions in the one-loop approximation can be found in Appendix G of Ref. [18].

With the $\overline{\text{MS}}$ coupling constant $\bar{g}$, we write the two-loop conversion matrix $C_{mm'}$ as

$$C_{mm'} = \delta_{mm'} + \frac{\bar{g}^2}{16\pi^2}(c_1)_{mm'} + \left(\frac{\bar{g}^2}{16\pi^2}\right)^2 (c_2)_{mm'}. \tag{B2}$$

For the multiplets $\mathscr{O}^{12}_{1}$ and $\mathscr{D}^{12}_{1}$, we have

$$C_{11}(\mathscr{O}^{12}_{1}) = C_{11}(\mathscr{D}^{12}_{1}), \tag{B3}$$

with

$$\begin{aligned} (c_1)_{11} &= -0.0493633154, \\ (c_2)_{11} &= -38.45080(90) + 3.746206(21)n_f. \end{aligned} \tag{B4}$$

In the case of the multiplet $\mathscr{S}^{4}_{1}$, one finds

$$\begin{aligned} (c_1)_{11} &= 2.629711269, \\ (c_2)_{11} &= 4.3294(24) + 0.004027(37)n_f. \end{aligned} \tag{B5}$$

The multiplets $\mathscr{O}^{4}_{\bar{1}}$ have a diagonal 2×2 mixing matrix with

$$\begin{aligned} (c_1)_{11} &= 2.629711269, \\ (c_2)_{11} &= 4.3294(24) + 0.004027(37)n_f, \\ (c_1)_{22} &= 2.629711269, \\ (c_2)_{22} &= 1.3116(24) + 0.004027(37)n_f. \end{aligned} \tag{B6}$$

For the multiplet $\mathscr{S}^{12}_{\bar{2}}$ of operators with one derivative, the conversion factor is given by

$$\begin{aligned} (c_1)_{11} &= -3.376398061, \\ (c_2)_{11} &= -105.555(12) + 11.076863(17)n_f. \end{aligned} \tag{B7}$$

The multiplets $\mathscr{O}^{12}_{\bar{2}}$ have a 4×4 mixing matrix with the diagonal entries

$$\begin{aligned} (c_1)_{11} &= 0.05197412907, \\ (c_2)_{11} &= -34.599(22) + 35.220102(34)n_f, \\ (c_1)_{22} &= -3.777434416, \\ (c_2)_{22} &= -109.878(12) + 11.563987(18)n_f, \\ (c_1)_{33} &= -3.376398061, \\ (c_2)_{33} &= -105.555(12) + 11.076863(17)n_f, \\ (c_1)_{44} &= -4.450577872, \\ (c_2)_{44} &= -114.543(13) + 12.620297(22)n_f. \end{aligned} \tag{B8}$$

The only nonvanishing off-diagonal entries are

$$\begin{aligned} (c_1)_{12} &= 0.05875235294, \\ (c_2)_{12} &= 1.8382(48) - 0.1089969(66)n_f, \\ (c_1)_{21} &= 0.2350094118, \\ (c_2)_{21} &= 7.858(10) - 0.4359875(86)n_f. \end{aligned} \tag{B9}$$

In the case of the multiplets $\mathscr{D}^{12}_{\bar{2}}$, we get a 3×3 mixing matrix, whose nonzero entries are given by

$$C_{mm'}(\mathscr{D}^{12}_{\bar{2}}) = C_{mm'}(\mathscr{O}^{12}_{\bar{2}}) \tag{B10}$$

for $m, m' \in \{1, 2\}$ and

$$\begin{aligned} (c_1)_{33} &= -1.388900608, \\ (c_2)_{33} &= -56.736(25) + 5.617296(39)n_f. \end{aligned} \tag{B11}$$

The uncertainties of the two-loop coefficients arising from the numerical evaluation of the master integrals have been estimated by error propagation. Since in this procedure possible correlations have been neglected, the given errors are most likely overestimated.

APPENDIX C: ANOMALOUS DIMENSIONS FOR GENERAL OPERATORS

Every local three-quark operator can be represented as a linear combination of the operators

$$\epsilon_{i_1 i_2 i_3}(D_{\bar{l}_1}\psi^{f_1}(x))^{i_1}_{\alpha_1}(D_{\bar{l}_2}\psi^{f_2}(x))^{i_2}_{\alpha_2}(D_{\bar{l}_3}\psi^{f_3}(x))^{i_3}_{\alpha_3}. \tag{C1}$$

Here, we use a multi-index notation for the covariant derivatives, $D_{\bar{l}} \equiv D_{\lambda_1}\cdots D_{\lambda_l}$. The indices $\alpha_1, \ldots$ are spinor indices, the indices $i_1, \ldots$ are color indices, and the flavor indices $f_1, \ldots$ take the values 1, 2, and 3, where $\psi^1 = u$, $\psi^2 = d$, and $\psi^3 = s$. In the context of renormalization, all flavors are taken to be massless. In the following, all quantities are to be understood as Euclidean.

The basic object for the renormalization of the local three-quark operators is the "flavorless" amputated four-point function

$$\begin{aligned} H^{\beta_1\beta_2\beta_3}_{\alpha_1\alpha_2\alpha_3}(\bar{l}_1,\bar{l}_2,\bar{l}_3;p_1,p_2,p_3) = -\int d^4x_1 d^4x_2 d^4x_3 e^{i(p_1\cdot x_1+p_2\cdot x_2+p_3\cdot x_3)}\epsilon_{j_1j_2j_3}\epsilon_{i_1i_2i_3} \\ \times\langle (D_{\bar{l}_1}u(0))^{j_1}_{\beta_1}(D_{\bar{l}_2}d(0))^{j_2}_{\beta_2}(D_{\bar{l}_3}s(0))^{j_3}_{\beta_3}\bar{u}^{i_1}_{\alpha'_1}(x_1)\bar{d}^{i_2}_{\alpha'_2}(x_2)\bar{s}^{i_3}_{\alpha'_3}(x_3)\rangle \\ \times G_2^{-1}(p_1)_{\alpha'_1\alpha_1}G_2^{-1}(p_2)_{\alpha'_2\alpha_2}G_2^{-1}(p_3)_{\alpha'_3\alpha_3}. \end{aligned} \tag{C2}$$

Here, $\langle\cdots\rangle$ indicates the functional integral with the gauge fields fixed, e.g., to Landau gauge, while p_1, p_2, and p_3 are the external momenta. The two-point function $G_2(p)$ required for the amputation is defined by

$$G_2(p)_{\alpha'\alpha}\delta_{ij} = \int d^4x e^{ip\cdot x}\langle u^j_{\alpha'}(0)\bar{u}^i_\alpha(x)\rangle. \tag{C3}$$

In the case of operators without derivatives, the renormalized (in the $\overline{\text{MS}}$-like scheme suggested in Ref. [11]) four-point function $\bar{H}^{\beta_1\beta_2\beta_3}_{\alpha_1\alpha_2\alpha_3}(-,-,-;p_1,p_2,p_3)$ is related to its bare counterpart by

$$\begin{aligned} &\bar{H}^{\beta_1\beta_2\beta_3}_{\alpha_1\alpha_2\alpha_3}(-,-,-;p_1,p_2,p_3) \\ &= Z_q^{-3/2}Z^{\beta_1\beta_2\beta_3}_{\beta'_1\beta'_2\beta'_3}H^{\beta'_1\beta'_2\beta'_3}_{\alpha_1\alpha_2\alpha_3}(-,-,-;p_1,p_2,p_3). \end{aligned} \tag{C4}$$

The matrix of anomalous dimensions can then be calculated as

$$\gamma = -\left(\mu\frac{dZ}{d\mu}\right)Z^{-1}. \tag{C5}$$

Here μ is the renormalization scale and Z_q is the wave function renormalization constant of the quark fields. With the $\overline{\text{MS}}$ coupling constant $\bar{g}$, the anomalous dimension can be written as

$$\gamma = \gamma_0\frac{\bar{g}^2}{16\pi^2} + \gamma_1\left(\frac{\bar{g}^2}{16\pi^2}\right)^2 + \cdots. \tag{C6}$$

The one-loop coefficient is given by

$$\gamma_0 = -\frac{1}{3}(G_{022}+G_{202}+G_{220}). \tag{C7}$$

The objects G_{022}, etc., carry six spinor indices like Z and are defined as

$$\begin{aligned} G_{022} &= \Gamma_0\otimes\Gamma_{\mu_1\mu_2}\otimes\Gamma_{\mu_1\mu_2}, \\ G_{202} &= \Gamma_{\mu_1\mu_2}\otimes\Gamma_0\otimes\Gamma_{\mu_1\mu_2}, \\ G_{220} &= \Gamma_{\mu_1\mu_2}\otimes\Gamma_{\mu_1\mu_2}\otimes\Gamma_0 \end{aligned} \tag{C8}$$

in terms of the totally antisymmetric products of γ matrices

$$\Gamma_0 = \mathbb{1}, \qquad \Gamma_{\mu\nu} = \frac{1}{2!}(\gamma_\mu\gamma_\nu - \gamma_\nu\gamma_\mu), \ldots \tag{C9}$$

Three-loop expressions for the anomalous dimensions of the operators without derivatives are given in Ref. [19].

For the operators with one derivative, the renormalization structure is more complicated. In addition to the matrix structure (encoded in the G_{lmn}) that operates on the open spinor indices, we have a 3×3 matrix structure, because the operators with the covariant derivative acting on the first, second, or third quark field mix with each other. Instead of Eq. (C4), we now have

$$\begin{pmatrix} \bar{H}^{\beta_1\beta_2\beta_3}_{\alpha_1\alpha_2\alpha_3}(\mu,-,-;p_1,p_2,p_3) \\ \bar{H}^{\beta_1\beta_2\beta_3}_{\alpha_1\alpha_2\alpha_3}(-,\mu,-;p_1,p_2,p_3) \\ \bar{H}^{\beta_1\beta_2\beta_3}_{\alpha_1\alpha_2\alpha_3}(-,-,\mu;p_1,p_2,p_3) \end{pmatrix} = Z_q^{-3/2} Z^{\beta_1\beta_2\beta_3}_{\beta_1'\beta_2'\beta_3'} \begin{pmatrix} H^{\beta_1'\beta_2'\beta_3'}_{\alpha_1\alpha_2\alpha_3}(\mu,-,-;p_1,p_2,p_3) \\ H^{\beta_1'\beta_2'\beta_3'}_{\alpha_1\alpha_2\alpha_3}(-,\mu,-;p_1,p_2,p_3) \\ H^{\beta_1'\beta_2'\beta_3'}_{\alpha_1\alpha_2\alpha_3}(-,-,\mu;p_1,p_2,p_3) \end{pmatrix}, \tag{C10}$$

where $Z^{\beta_1\beta_2\beta_3}_{\beta_1'\beta_2'\beta_3'}$ is a 3×3 matrix. The one-loop contribution to the matrix of anomalous dimensions for operators of leading twist is given by

$$\gamma_0 = \begin{pmatrix} 32/9 & -16/9 & -16/9 \\ -16/9 & 32/9 & -16/9 \\ -16/9 & -16/9 & 32/9 \end{pmatrix} \otimes G_{000} + \begin{pmatrix} -1/3 & 0 & 0 \\ 0 & -2/9 & -1/9 \\ 0 & -1/9 & -2/9 \end{pmatrix} \otimes G_{022} + \begin{pmatrix} -2/9 & 0 & -1/9 \\ 0 & -1/3 & 0 \\ -1/9 & 0 & -2/9 \end{pmatrix} \otimes G_{202} + \begin{pmatrix} -2/9 & -1/9 & 0 \\ -1/9 & -2/9 & 0 \\ 0 & 0 & -1/3 \end{pmatrix} \otimes G_{220}. \tag{C11}$$

The two-loop contribution, again projected onto leading twist, reads

$$\begin{aligned} \gamma_1 = {} & \begin{pmatrix} 8348/81-(508/81)n_f & -1339/81+(92/81)n_f & -1339/81+(92/81)n_f \\ -1339/81+(92/81)n_f & 8348/81-(508/81)n_f & -1339/81+(92/81)n_f \\ -1339/81+(92/81)n_f & -1339/81+(92/81)n_f & 8348/81-(508/81)n_f \end{pmatrix} \otimes G_{000} \\ & + \begin{pmatrix} -1265/486+(1/27)n_f & -55/243 & -55/243 \\ -29/486 & -817/486+(4/81)n_f & -22/27-(1/81)n_f \\ -29/486 & -22/27-(1/81)n_f & -817/486+(4/81)n_f \end{pmatrix} \otimes G_{022} \\ & + \begin{pmatrix} -817/486+(4/81)n_f & -29/486 & -22/27-(1/81)n_f \\ -55/243 & -1265/486+(1/27)n_f & -55/243 \\ -22/27-(1/81)n_f & -29/486 & -817/486+(4/81)n_f \end{pmatrix} \otimes G_{202} \\ & + \begin{pmatrix} -817/486+(4/81)n_f & -22/27-(1/81)n_f & -29/486 \\ -22/27-(1/81)n_f & -817/486+(4/81)n_f & -29/486 \\ -55/243 & -55/243 & -1265/486+(1/27)n_f \end{pmatrix} \otimes G_{220} \\ & + \begin{pmatrix} 1/9 & 0 & 0 \\ 0 & 109/1944 & 107/1944 \\ 0 & 107/1944 & 109/1944 \end{pmatrix} \otimes G_{044} + \begin{pmatrix} 109/1944 & 0 & 107/1944 \\ 0 & 1/9 & 0 \\ 107/1944 & 0 & 109/1944 \end{pmatrix} \otimes G_{404} \\ & + \begin{pmatrix} 109/1944 & 107/1944 & 0 \\ 107/1944 & 109/1944 & 0 \\ 0 & 0 & 1/9 \end{pmatrix} \otimes G_{440} \\ & + \begin{pmatrix} -4/243 & -5/486 & -5/486 \\ -19/972 & -1/27 & -2/243 \\ -19/972 & -2/243 & -1/27 \end{pmatrix} \otimes G_{422} + \begin{pmatrix} -1/27 & -19/972 & -2/243 \\ -5/486 & -4/243 & -5/486 \\ -2/243 & -19/972 & -1/27 \end{pmatrix} \otimes G_{242} \\ & + \begin{pmatrix} -1/27 & -2/243 & -19/972 \\ -2/243 & -1/27 & -19/972 \\ -5/486 & -5/486 & -4/243 \end{pmatrix} \otimes G_{224} + \begin{pmatrix} 0 & 2/81 & -2/81 \\ -2/81 & 0 & 2/81 \\ 2/81 & -2/81 & 0 \end{pmatrix} \otimes G_{222}. \end{aligned} \tag{C12}$$

The one-loop anomalous dimension matrix (C11) was first presented in this form in Ref. [33], unfortunately with some typos. However, the analysis code employed in Refs. [1,2,18] was correct. The two-loop result in (C12) is new. Notice that the anomalous dimensions (C7), (C11), and (C12) are not only relevant for spin 1/2 baryons, but also for spin 3/2 baryons.

APPENDIX D: ANOMALOUS DIMENSIONS FOR LATTICE OPERATORS

The lattice operators (or rather operator multiplets) that are relevant for the evaluation of (moments of) baryon DAs can be found in Appendix A. In Appendix E of Ref. [18], the three-loop anomalous dimensions of the operators without derivatives are given, derived from the results in Ref. [19]. Here we present the new two-loop anomalous dimensions of the operators with one derivative.

For the multiplet $\mathscr{S}^{12}_{2}$, we get

$$\gamma_0 = \frac{52}{9},$$
$$\gamma_1 = \frac{28990}{243} - \frac{620}{81} n_f. \tag{D1}$$

In the case of the four mixing multiplets $(\mathscr{O}^{12}_{2})_1, \ldots, (\mathscr{O}^{12}_{2})_4$, one finds

$$\gamma_0 = \begin{pmatrix} 4/3 & 0 & 0 & 0 \\ 0 & 20/3 & 0 & 0 \\ 0 & 0 & 52/9 & 0 \\ 0 & 0 & 0 & 8 \end{pmatrix},$$
$$\gamma_1 = \begin{pmatrix} 236/3 - 112n_f/27 & -16\sqrt{2}/27 & 0 & 0 \\ 0 & 1174/9 - 68n_f/9 & 0 & 0 \\ 0 & 0 & 28990/243 - 620n_f/81 & 0 \\ 0 & 0 & 0 & 428/3 - 8n_f \end{pmatrix}. \tag{D2}$$

Finally, we have the three mixing multiplets $(\mathscr{D}^{12}_{2})_1, \ldots, (\mathscr{D}^{12}_{2})_3$ with

$$\gamma_0 = \begin{pmatrix} 4/3 & 0 & 0 \\ 0 & 20/3 & 0 \\ 0 & 0 & 4 \end{pmatrix}, \qquad \gamma_1 = \begin{pmatrix} 236/3 - 112n_f/27 & -16\sqrt{2}/27 & 0 \\ 0 & 1174/9 - 68n_f/9 & 0 \\ 0 & 0 & 328/3 - 40n_f/9 \end{pmatrix}. \tag{D3}$$

APPENDIX E: COMPARING ONE-LOOP AND TWO-LOOP CONVERSION

In this appendix, we present some plots directly comparing renormalization factors obtained with one-loop and two-loop conversion. We do this for the multiplets $\mathscr{O}^{12}_{1}$ (Fig. 5) and $\mathscr{S}^{12}_{2}$ (Fig. 6), separately for our coarsest ($a^{-1} \approx 2.3$ GeV, $\beta = 3.4$) and finest ($a^{-1} \approx 5.1$ GeV, $\beta = 3.85$) lattices. Notice that these data are included in Figs. 2 and 4.

Replacing one-loop by two-loop conversion leads to larger effects for the multiplet $\mathscr{S}^{12}_{2}$ of operators with one derivative than for the multiplet $\mathscr{O}^{12}_{1}$ of operators without derivatives. Still, in the relevant range of scales around $\mu^2 = 4$ GeV^2, these effects are of moderate size (∼1.5% for $\mathscr{O}^{12}_{1}$ and ∼4.5% for $\mathscr{S}^{12}_{2}$), and the uncertainties due to the perturbative conversion are not the major source of systematic errors of our final results.

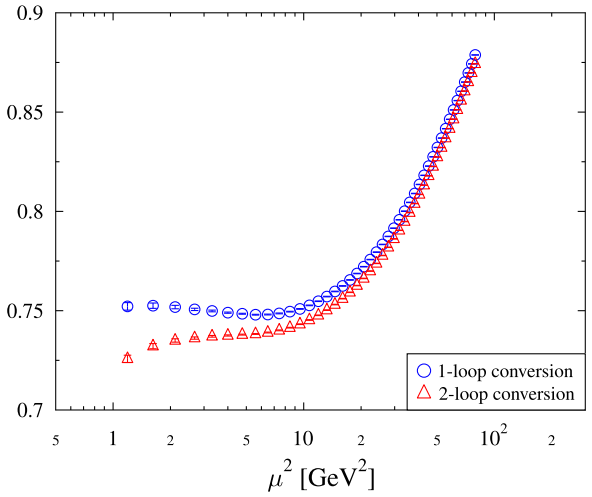

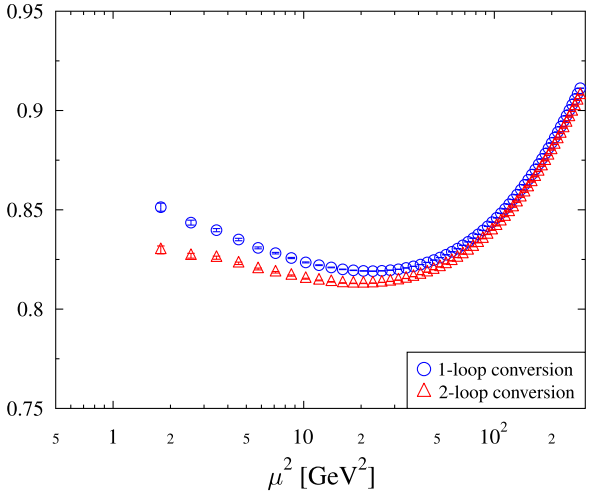

FIG. 5. Renormalization factor for the multiplet $\mathscr{O}_1^{12}$ rescaled to the target scale of 2 GeV for $\beta = 3.4$ (top panel) and $\beta = 3.85$ (bottom panel).

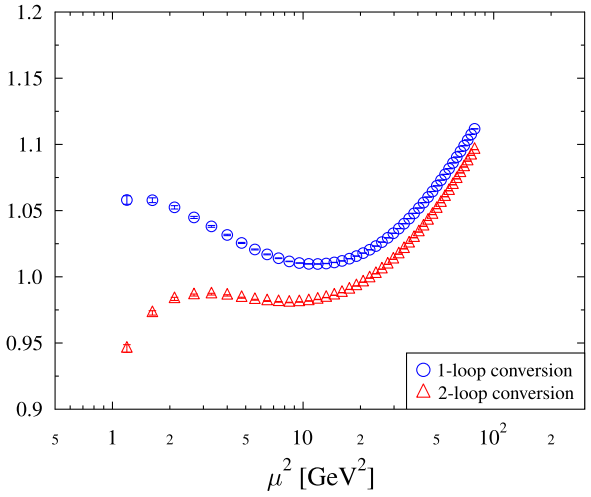

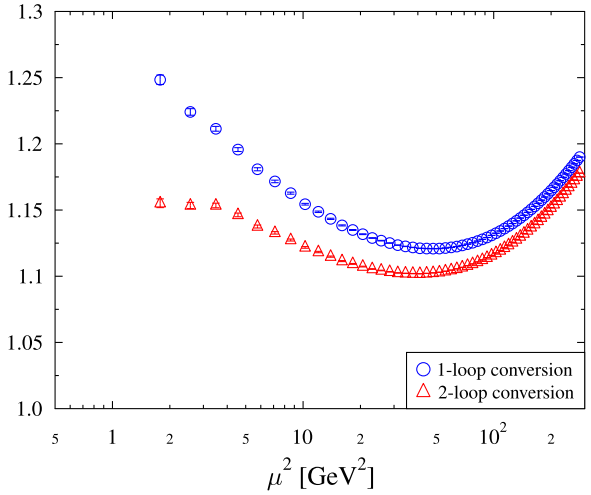

FIG. 6. Renormalization factor for the multiplet $\mathscr{S}_2^{12}$ rescaled to the target scale of 2 GeV for $\beta = 3.4$ (top panel) and $\beta = 3.85$ (bottom panel).

[1] G. S. Bali *et al.* (RQCD Collaboration), Light-cone distribution amplitudes of octet baryons from lattice QCD, Eur. Phys. J. A **55**, 116 (2019).

[2] G. S. Bali *et al.*, Light-cone distribution amplitudes of the baryon octet, J. High Energy Phys. 02 (2016) 070.

[3] Z. F. Deng, C. Han, W. Wang, J. Zeng, and J. L. Zhang, Light-cone distribution amplitudes of a light baryon in large-momentum effective theory, J. High Energy Phys. 07 (2023) 191.

[4] C. Han, Y. Su, W. Wang, and J. L. Zhang, Hybrid renormalization for quasi distribution amplitudes of a light baryon, J. High Energy Phys. 12 (2023) 044.

[5] C. Han and J. Zhang, Light baryon spatial correlators at short distances, Phys. Rev. D **109**, 014034 (2024).

[6] C. Han, W. Wang, J. Zeng, and J. L. Zhang, Lightcone and quasi distribution amplitudes for light octet and decuplet baryons, J. High Energy Phys. 07 (2024) 019.

[7] W. Chen, F. Feng, and Y. Jia, Next-to-leading-order QCD corrections to nucleon Dirac form factors, arXiv:2406.19994.

[8] Y. K. Huang, B. X. Shi, Y. M. Wang, and X. C. Zhao, Next-to-leading-order QCD predictions for the nucleon form factors, arXiv:2407.18724.

[9] M. H. Chu *et al.*, Light cone distribution amplitude for the Λ baryon from lattice QCD, Phys. Rev. D **111**, 034510 (2025).

[10] B. A. Kniehl and O. L. Veretin, Renormalization of three-quark operators at two loops in the RI'/SMOM scheme, Nucl. Phys. **B992**, 116210 (2023).
[11] S. Kränkl and A. Manashov, Two-loop renormalization of three-quark operators in QCD, Phys. Lett. B **703**, 519 (2011).
[12] V. Braun, R. J. Fries, N. Mahnke, and E. Stein, Higher twist distribution amplitudes of the nucleon in QCD, Nucl. Phys. **B589**, 381 (2000); Nucl. Phys. **B607**, 433(E) (2001).
[13] V. M. Braun, A. N. Manashov, and J. Rohrwild, Baryon operators of higher twist in QCD and nucleon distribution amplitudes, Nucl. Phys. **B807**, 89 (2009).
[14] V. L. Chernyak and A. R. Zhitnitsky, Asymptotic behavior of exclusive processes in QCD, Phys. Rep. **112**, 173 (1984).
[15] M. Bruno *et al.*, Simulation of QCD with $N_f = 2 + 1$ flavors of non-perturbatively improved Wilson fermions, J. High Energy Phys. 02 (2015) 043.
[16] G. S. Bali, S. Collins, P. Georg, D. Jenkins, P. Korcyl, A. Schäfer, E. E. Scholz, J. Simeth, W. Söldner, and S. Weishäupl (RQCD Collaboration), Scale setting and the light baryon spectrum in $N_f = 2 + 1$ QCD with Wilson fermions, J. High Energy Phys. 05 (2023) 035.
[17] M. Bruno, M. Dalla Brida, P. Fritzsch, T. Korzec, A. Ramos, S. Schaefer, Hubert Simma, Stefan Sint, and R. Sommer (ALPHA Collaboration), QCD coupling from a nonperturbative determination of the three-flavor Λ parameter, Phys. Rev. Lett. **119**, 102001 (2017).
[18] G. S. Bali, S. Bürger, S. Collins, M. Göckeler, M. Gruber, S. Piemonte, A. Schäfer, A. Sternbeck, and P. Wein (RQCD Collaboration), Nonperturbative renormalization in lattice QCD with three flavors of clover fermions: Using periodic and open boundary conditions, Phys. Rev. D **103**, 094511 (2021); Phys. Rev. D **107**, 039901(E) (2023).
[19] J. A. Gracey, Three-loop renormalization of 3-quark operators in QCD, J. High Energy Phys. 09 (2012) 052.
[20] T. Ledwig, J. Martin Camalich, L. S. Geng, and M. J. Vicente Vacas, Octet-baryon axial-vector charges and $SU(3)$-breaking effects in the semileptonic hyperon decays, Phys. Rev. D **90**, 054502 (2014).
[21] G. S. Bali, V. M. Braun, S. Bürger, M. Göckeler, M. Gruber, F. Hutzler, P. Korcyl, A. Schäfer, A. Sternbeck, and P. Wein (RQCD Collaboration), Light-cone distribution amplitudes of pseudoscalar mesons from lattice QCD, J. High Energy Phys. 08 (2019) 065; J. High Energy Phys. 11 (2020) 037.
[22] R. G. Edwards and B. Joó (SciDAC, LHPC, and UKQCD Collaborations), The CHROMA software system for lattice QCD, Nucl. Phys. B, Proc. Suppl. **140**, 832 (2005).
[23] A. Nobile, Solving the Dirac equation on QPACE, Proc. Sci. LATTICE2010 (**2010**) 034.
[24] M. Lüscher and S. Schaefer, Lattice QCD with open boundary conditions and twisted-mass reweighting, Comput. Phys. Commun. **184**, 519 (2013).
[25] A. Frommer, K. Kahl, S. Krieg, B. Leder, and M. Rottmann, Adaptive aggregation-based domain decomposition multigrid for the lattice Wilson–Dirac operator, SIAM J. Sci. Comput. **36**, A1581 (2014).
[26] S. Heybrock, M. Rottmann, P. Georg, and T. Wettig, Adaptive algebraic multigrid on SIMD architectures, Proc. Sci. LATTICE2015 (**2016**) 036.
[27] G. S. Bali, E. E. Scholz, J. Simeth, and W. Söldner (RQCD Collaboration), Lattice simulations with $N_f = 2 + 1$ improved Wilson fermions at a fixed strange quark mass, Phys. Rev. D **94**, 074501 (2016).
[28] https://luscher.web.cern.ch/luscher/openQCD/
[29] Jülich Supercomputing Centre, JURECA: Modular supercomputer at Jülich Supercomputing Centre, J. Large-Scale Res. Facil. **4**, A132 (2018).
[30] http://www.fz-juelich.de/ias/jsc/
[31] Jülich Supercomputing Centre, JUWELS: Modular tier-0/1 supercomputer at the Jülich Supercomputing Centre, J. Large-Scale Res. Facil. **5**, A135 (2019).
[32] T. Kaltenbrunner, M. Göckeler, and A. Schäfer, Irreducible multiplets of three-quark operators on the lattice: Controlling mixing under renormalization, Eur. Phys. J. C **55**, 387 (2008).
[33] M. Gruber, Renormalization of three-quark operators for baryon distribution amplitudes, Ph.D. thesis, Universität Regensburg, Germany, 2017, http://nbn-resolving.org/urn:nbn:de:bvb:355-epub-364421.